Summer Student Project Summary

TRACK STUDIES WITH THE ITS INNER BARREL

Agnese Spustaka

Supervisors: Magnus Mager and Jochen Klein, EP-AID-DT&EP-AIP-PAP, CERN

Abstract

In July 2022, Run 3 at the CERN LHC (Large Hadron Collider) began. ALICE (A Large Ion Collider Experiment) underwent significant improvements in order to get ready for this new data collection phase, one of which was upgrade of the ITS (Inner Tracking System). In this project, data from the ITS inner barrel is used to study noisy pixels, cluster size, vertex position, and associated tracks. The residuals of the fitting were analysed. With the available data and precision, no significant correlation of cluster size and residuals could be found.

Contents

1. Introduction
1.1 ALICE

A general-purpose heavy-ion detector called ALICE (A Large Ion Collider Experiment) is located at CERN's Large Hadron Collider (LHC) and is schematically visualized in Figure 1. The goal of ALICE is to study the physics of strongly interacting matter, specifically the characteristics of the quark-gluon plasma (QGP). The LHC began a two-year upgrade phase known as the Long Shutdown 2 in December 2018, ending the four-year Run 2 period of operation (LS2). Improvements implemented to the accelerator complex during LS2 boost the heavy-ion collision parameters of Run 3 and 4 to well beyond the specifications of the previous ALICE setup. During the LS2, a number of improvements at ALICE were made including the installation of three new detectors: the new Inner Tracking System (ITS), the new Muon Forward Tracker (MFT), and the new Fast Interaction detector. This was done in order to adapt to such a significant change in the running conditions and to accomplish the proposed physics objectives.[1]

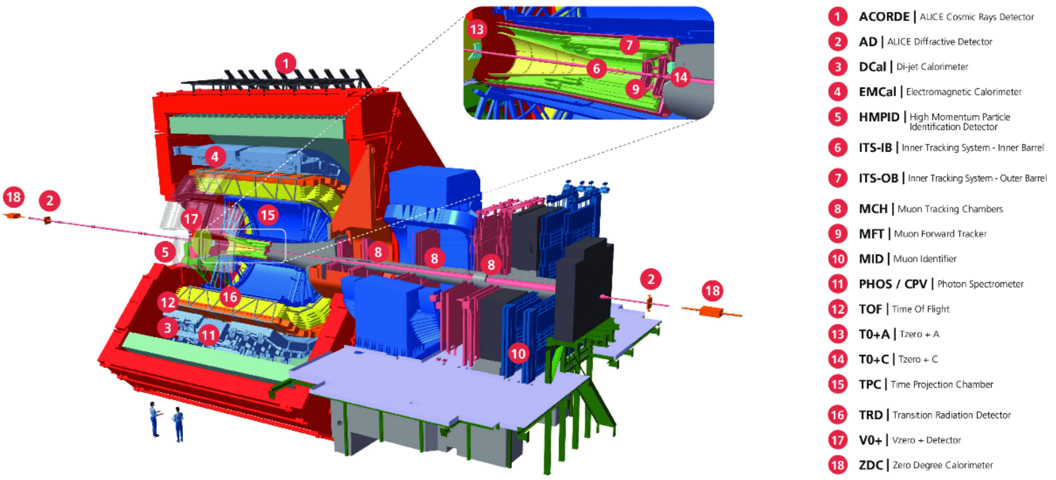

Figure 1. *Schematical illustration of the ALICE setup for LHC Run 3.*

1.2 ITS upgrade

Compared to the silicon tracker used during Runs 1 and 2, the new ITS is a significant advancement. There are seven sensor layers surrounding the beam (*Figure 2*) up from six, with the innermost layer being 23 mm from the beam axis, which is much closer than the previous system's 39 mm inner radius. The three innermost layers are referred to as Inner Barrel (IB), while the four outer layers are referred to as Outer Barrel (OB).[2]

The pseudorapidity η coverage of the tracker is increased from $-1 \leq \eta \leq 1$ to $-1.5 \leq \eta \leq 1.5$. In comparison to the original ITS's 6 m^2, the active silicon area now is increase to 10 m^2. Due to the characteristics of ALPIDE [3], the spatial resolution is 5×5 μm^2. The previous ITS used three detector technologies – pixel detectors, drift detectors and strip detectors. The spatial resolution was, respectively, 12×100 μm^2, 35×35 μm^2 and 20×830 μm^2.

The smaller pixel size will result in an improvement in pointing resolution along the beam direction by a factor of 6 and by a factor of 3 improvement in the r φ direction, with a 40 μm resolution at $p_T = 500$ MeV/c. The previous ITS could readout data at a maximum rate of just 1 kHz. Now it will be increased up to 100 kHz for Pb–Pb collisions and up to 1 MHz for pp.[1]

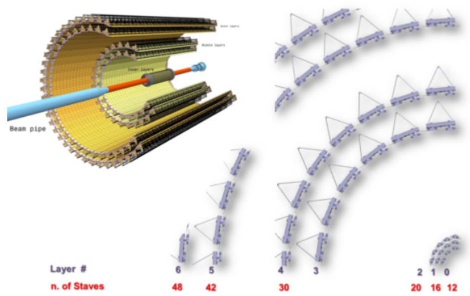

Figure 2. *Schematic view of upgraded ITS [4].*

2 Dataset

In this project data from ITS inner barrel layers is used to analyse the correlation between low and high momentum particles and the corresponding size of the residuals of track fitting. The data was taken during the pilot beam in 2021.

When charged particles go through the detector chips, pixels near the intersection point of the particle track and detector fire. Particles with low momenta tend to lose more energy thus typically more pixels fire, while particles with high momenta tend to fire fewer number of pixels.

The provided *json* file contains data about 100 collision events, each event is represented by fired clusters. Each cluster includes information about chip [half, layer, stave, chip number] where pixel [row, column] was fired, example in *Figure 3*.


```
{"clusters":
[{"chip": [1, 2, 6, 3], "pixels": [[671, 447], [671, 446]]},
{"chip": [0, 0, 4, 7], "pixels": [[368, 43], [367, 43], [366, 43], [365, 43], [366, 42], [367, 42], [368, 42]]},
{"chip": [0, 2, 2, 0], "pixels": [[221, 317], [220, 317], [219, 317], [218, 317], [219, 316]]}],
"evno": 156},
```


Figure 3. *Data format in json file.*

The detector is installed in two halves, named top and bottom. Information about number of staves and chips in every half is summarised in *Table 1.*

Layer	R, *mm*	Staves, #	Chips, #
0	23	6	54
1	31	8	72
2	39	10	90

Table 1. *Technical data about number of chips in each half of ITS IB.*

3 Data analysis

Data analysis has been done using *Jupyter Notebook* with *python3.6.9*, explicitly using *json, linalg, matplotlib, numpy*, *pandas*, and *sympy* packages. To find tracks and analyse residuals it is important that there is a low number of noisy pixels. It was found that there are only 3 noisy pixels out of more than 226 million pixels in the detector. These pixels fired on their own and typically were not included in clusters. These pixels were removed from further analysis.

Clusters are made of fired pixels representing a point where particle crossed the detector, to find a track, only point that represents a centre of mass of cluster is used. For further processing of data, the fired pixels' locations from layer, stave and chip coordinates were transformer to global x, y, z coordinate system, where the z axis is along the beam. This was done using 4D projective geometry where 5 different matrixes, three for rotating in each of directions (x, y, z), one for translations, and one for scaling are used for any possible transformation. Total transformation matrix is obtained by multiplying the necessary elementary transformations, then data point using only pixel's row and column could be multiplied with transformation matrix to get the new coordinates in x, y, z.

New variables were introduced for a better understanding of the data and the underlying physical processes. To describe the distance from the beam, a radius r was introduced in the plane perpendicular to the beam, given by $r = \sqrt{x^2 + y^2}$, φ describes the angle between x and y and is given by $\varphi = \tan^{-1}\left(\frac{y}{x}\right)$, while θ describes the angle to describe angle between z axis and r as $\theta = \tan^{-1}\left(\frac{r}{z}\right)$. Additionally, to describe the angle of the particle relative of beam axis, pseudorapidity was introduced as $\eta = -\ln\left[tan\left(\frac{\theta}{2}\right)\right]$.

The particles going through the first layers of the detector tend to cross it in a straight line, example of one of the events in *Figure 4*. Here one can see a typical event in respect of different variables that were introduced previously.

3.1 Track finding and fitting

Before finding tracks of particles, possible track candidates were grouped together in terms of angle φ. The optimal angle interval was 2˚, this diapason was found using trial and error. First, the track and its vertex were found in Z-R

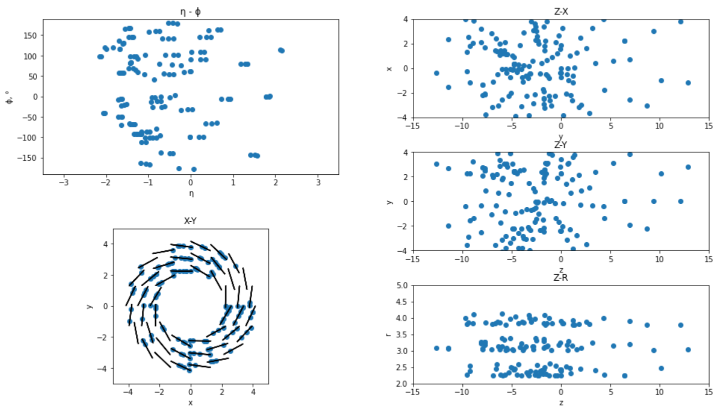

Figure 4. *Example of fired clusters in one event in respect of different variables, blue dots – fired clusters, black lines – detector.*

coordinates. The line that best characterize possible track candidates was found using a least squares approach. After this step was completed, there were still tracks that poorly described the data, so these points and their respective track lines were not taken in account further. To find the potential vertex position, it was approximated that $r = 0$. In Figure 5 one can see that the line tracks tend to intersect in one point. In the a) graph, black points and grey lines correspond outliers that later are excluded, in the b) graph, no outliers can be seen. The vertex position is shown in title, all values are in cm, in c) there can be seen histogram of z vertex positions, showing that all collisions were not in the centre of detector.

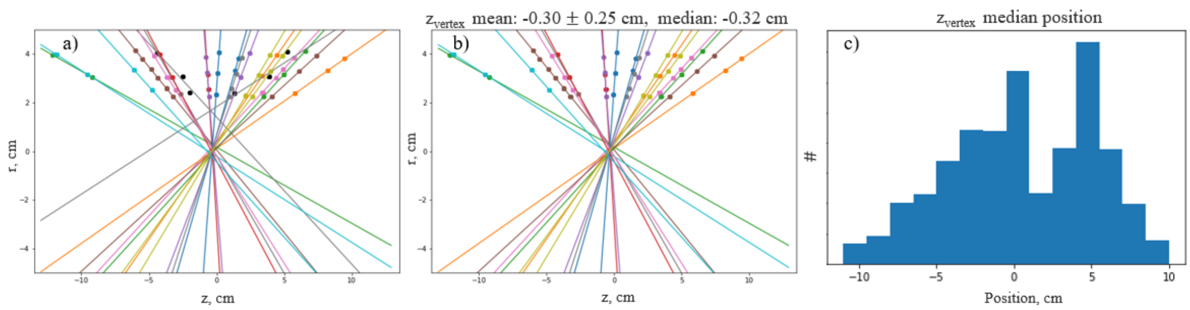

Figure 5. *Tracks in Z-R coordinates – a) with outliers, b) without outliers; c) histogram of z vertex position.*

Possible track candidates after 2D approximation were plotted in 3D. Then using principal component analysis the 3D line for the track was found. Data points are defined as $x_1, \ldots, x_n \in \mathbb{R}^3$. In $\mathbb{R}^3$ a line can be defined as $\vec{\ell} = \vec{\bar{x}} + \vec{n}t$: $t \in \mathbb{R}$, where $\vec{\bar{x}}$ is centre of mass of data point and $\vec{n}$ is line direction vector. To find line direction vector $\vec{n}$, one can solve eigen problem for the covariance matrix. First, de-mean data points as $x_i \leftarrow x_i - \bar{x}$, then find covariance matrix M as $M = \frac{1}{n}\sum_{i=1}^{n} x_i x_i^T$. Then finding eigenvector $\vec{n}$ corresponding to the largest eigenvalue of M. The result of 3D line fitting can be seen in *Figure 6*. In the left graph, an event with numerous tracks that tends to one point can be seen, while in the right graph only few tracks crossing the detector chip plane are seen.

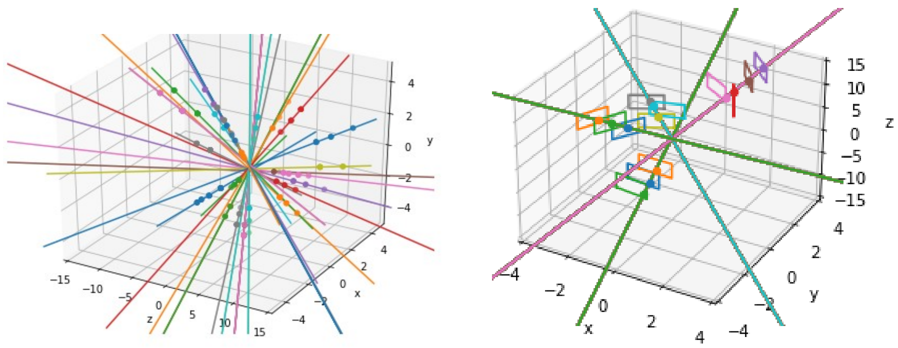

Figure 6. *3D line fit using PCA, left – event with numerous tracks, right – event with few tracks with detector chips shown.*

3.2 Residuals

To estimate the quality of track fitting, residuals were introduced. Two different approaches were used. In global coordinates x, y, z the residuals were calculated using the closest point on the track's line. Point on the line is defined as $\vec{r_c} = \vec{r_0} + t_{min}\vec{n}$. The closest point could be found by minimizing t. The residuals in global coordinates are defined as $\vec{res} = \vec{x} - \vec{r_c}$.

To find residuals in detector's chip coordinates, the intersection point of track and detector plane was found $\vec{r_d}$, the residuals were found as $\vec{res} = \vec{x} - \vec{r_d}$. Each detector plane could be described with two vectors: $\vec{a} = (0, 0, z)$ and $\vec{b} = (x, y, 0)$, schematical illustration in *Figure 7*. Residuals were evaluated as projections on vectors $\vec{a}$ and $\vec{b}$ to avoid differences in x, y only because of alignment of pixels' chips.

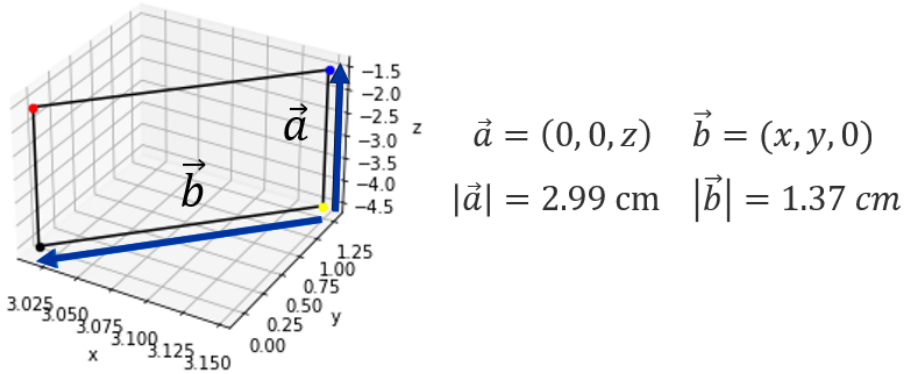

Figure 7. *Schematical illustration of detector in global coordinates (x, y, z).*

4 Results

To evaluate the quality of fits, the histograms of residuals in terms of projection on vectors that responds to pixels' chip were analysed (*Figure 8.* Residuals plots as projections on $\vec{a}$ and $\vec{b}$.). One can see that both histograms are unimodal with centre around 0. However, the widths of distribution are different, showing that in z direction there was more uncertainties.

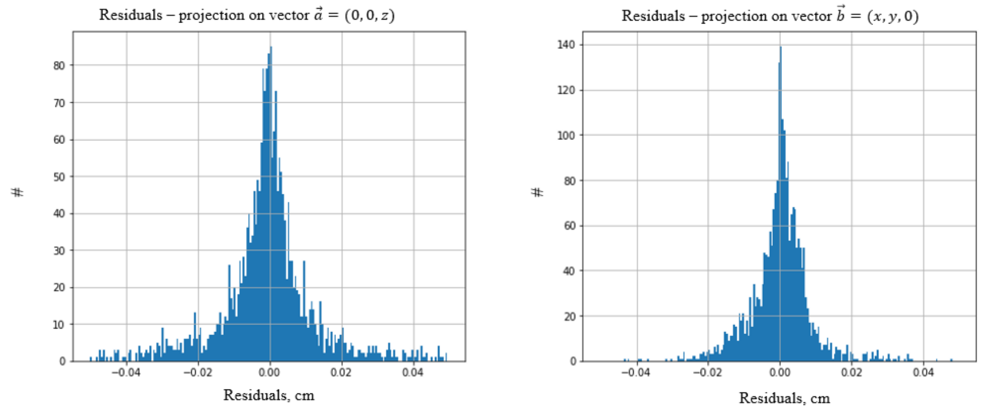

Figure 8. *Residuals plots as projections on $\vec{a}$ and $\vec{b}$.*

To analyse the relation between particles' momenta and the corresponding residual value, the cluster sizes and respective residual values were plotted in *Figure 9.* Presumption that particles with lower energy deposit more energy thus cluster size, and consequently, the fit residuals are larger. This could not be confirmed as the uncertainties do not allow to conclude that from *Figure 9 (c), d)).*

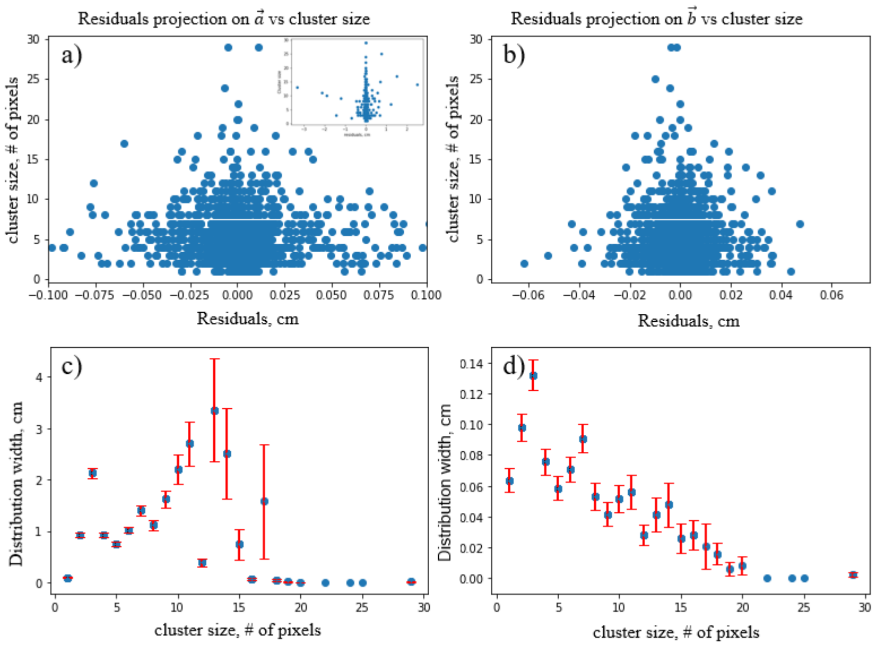

Figure 9. *a) Residuals projections on vector $\vec{a}$, b) on vector $\vec{b}$. Distribution width dependence of cluster size c) from the projections on $\vec{a}$, d) from the projections on $\vec{b}$.*

5 Summary

- The data collected during the pilot beam from the inner barrel of ALICE's upgraded inner tracking system was used to study noisy pixels, cluster size, vertex position, and associated tracks. The residuals of the fitting were analysed.

- It is known that when more energy is deposited by the lower energy particles, the cluster size will increase, which would also cause increase the size of the fit residuals. The uncertainties prevent drawing that conclusion from our results.

- To investigate further one could in the future look at the detector alignment positions, analysing the residuals respective to layers, staves, and chip positions.

6 References

[1] Trzaska, W. H. (2020). New ALICE detectors for Run 3 and 4 at the CERN LHC. *Nuclear Instruments and Methods in Physics Research Section A: Accelerators, Spectrometers, Detectors and Associated Equipment*, *958*, 162116.

[2] Abelev, B. (2014). Technical Design Report for the Upgrade of the ALICE Inner Tracking System. *Journal of Physics G: Nuclear and Particle Physics*, *41*(8), 87002.

[3] Aglieri Rinella, G. (2017). The ALPIDE pixel sensor chip for the upgrade of the ALICE Inner Tracking System. *Nuclear Instruments and Methods in Physics Research Section A: Accelerators, Spectrometers, Detectors and Associated Equipment*, *845*, 583–587.

[4] Martinengo, P. (2017). The new Inner Tracking System of the ALICE experiment. *Nuclear Physics A*, *967*, 900–903.